Hz), 74.2, 71.7, 69.6 (d, J = 9.9 Hz), 69.3, 68.8, 66.8, 64.8 (d, J = 5.3 Hz), 63.0, 51.8, 41.1 (d, J = 9.7 Hz), 22.1.

Purification of CMP-NeuAc: Differential Precipitation. CMP-NeuAc was generated as described above except that the NeuAc (1 g) used had been purified by ion-exchange chromatography. The following steps were performed at 4 °C. The reaction mixture was centrifuged (25000g, 20 min), and the pellet was resuspended in 100 mL of 10 mM NH_4OH and centrifuged again. This wash procedure was repeated. Combination of the washings and dialysates (see above) yielded a solution whose pH was adjusted to pH 9.5 and was then concentrated; the pH must be checked when the volume is approximately halved and adjusted up to pH 9 during this step to prevent hydrolysis. The concentrate was desalted on Biogel P-2 (100 × 4.5 cm; eluant, 10 mM NH_4OH), and the fractions containing CMP-NeuAc (determined by TLC as above) were pooled and concentrated to 30 mL. Slow addition of ethanol (30 mL) precipitated CTP, and the solution was centrifuged (10000g, 10 min). The supernatant containing CMP-NeuAc was decanted, and the pellet was resuspended in 30 mL of 10 mM NH_4OH. The precipitation and centrifugation steps were repeated. The combined supernatants were concentrated to near dryness and redissolved in 50 mL of 10 mM NH_4OH. The pH of the solution was adjusted to pH 9, and alkaline phosphatase (~200 U) and $MgCl_2 \cdot 6H_2O$ (1.1 g) was added as above. After 90 min, the pH of the solution was adjusted to 9.5 and the solution was centrifuged (10000g, 10 min). The supernatant was saved, the pellet was resuspended in 25 mL of 10 mM NH_4OH, and the solution was centrifuged again. This wash procedure was repeated. The combined supernatants were concentrated to 30 mL, and the addition of ethanol (270 mL) precipitated **5**. The supernatant was concentrated to 30 mL, and the precipitation was repeated. The collected precipitates were desalted on Biogel P-2 as above to yield 1.2 g of a solid containing ~90% CMP-NeuAc (~50% yield from **2**); pyruvate, dipyruvate, and an unidentified contaminant were also present.

(5-Acetamido-1-carboxy-3,5-dideoxy-α-D-*glycero*-D-*galacto*-2-nonulopyranosyl)-(2,6)-β-D-galactopyranosyl-(1,4)-2-acetamido-2-deoxy-α,β-D-glucopyranose (2,6-Sialyllactosamine, 6). A solution of 43 mg of sodium cacodylate (200 μmol), 10 mg of CMP-NeuAc (14 μmol), and 17 mg of *N*-acetyllactosamine (43 μmol; synthesized from glucose[62]) in 2 mL of D_2O was placed in a plastic, 15-mL polypropylene tube. Addition of 0.4 N HCl in D_2O adjusted the solution to pH 6.8, 0.1 mL (~17 mU) of 2,6-sialyltransferase was added, and the tube was capped and left at room temperature. ^1H NMR spectroscopy (500 MHz) indicated that the reaction was >90% complete after 2 days. Purification by ion-exchange chromatography[11] yielded ~3 mg (4 μmol) of **6**, identified by comparison of its ^1H NMR spectrum to that reported in the literature.[11]

(5-Acetamido-1-carboxy-3,5-dideoxy-α-D-*glycero*-D-*galacto*-2-nonulopyranosyl)-(2,6)-β-D-galactopyranosyl-(1,4)-α,β-D-glucopyranose (2,6-Sialyllactose, 7). A solution of 43 mg of sodium cacodylate (200 μmol), 10 mg of CMP-NeuAc (14 μmol), and 800 mg of lactose (155 μmol) in 2 mL of D_2O was placed in a plastic, 15-mL polypropylene tube. Addition of 0.4 N HCl in D_2O adjusted the solution to pH 6.8, 0.1 mL (~17 mU) of 2,6-sialyltransferase was added, and the tube was capped and left at room temperature. ^1H NMR spectroscopy (500 MHz) indicated that the reaction was 50% complete after 1 week. Purification by ion-exchange chromatography[11] yielded ~1 mg (2 μmol) of **7**, identified by comparison of its ^1H NMR spectrum to that reported in the literature.[11]

Registry No. 1, 7512-17-6; **2**, 3615-17-6; **3**, 131-48-6; **5**, 3063-71-6; **6**, 78969-47-8; **7**, 35890-39-2; CTP, 65-47-4; CMP, 63-37-6; CDP, 63-38-7; *N*-acetyllactosamine, 32181-59-2; lactose, 63-42-3; adenylate kinase, 9013-02-9; pyruvate kinase, 9001-59-6; acetylneuraminic acid aldolase, 9027-60-5; CMP-acetylneuraminic acid synthetase, 9067-82-7; 2,6-sialyltransferase, 9075-81-4.

(62) Wong, C.-H.; Haynie, S. L.; Whitesides, G. M. *J. Org. Chem.* **1982**, *47*, 5416.

Photophysics, Photochemistry, and Theoretical Calculations of Some Benz[*a*]anthracene-3,4-diones and Their Significance

Ralph S. Becker,*,† L. V. Natarajan,† Christian Lenoble,† and Ronald G. Harvey‡

Contribution from the Department of Chemistry, University of Houston, Houston, Texas 77004, and Ben May Institute, University of Chicago, Chicago, Illinois 60637.
Received January 6, 1988. Revised Manuscript Received May 19, 1988

Abstract: The unsubstituted benz[*a*]anthracene-3,4-dione (*o*-quinone) and various 7- and 12-methyl-substituted benz[*a*]-anthracene-3,4-diones have been studied in detail. All these quinones have a lowest energy absorption band corresponding to n → π* singlet transition. Theoretical calculations employing the INDO method for the spin-allowed transitions of both n,π* and π,π* types are in good agreement with those experimentally observed. Laser flash photolyses of all these quinones show the presence of a triplet transient, with the difference absorption spectrum showing a high-intensity maximum around 800 nm. All the above quinones exhibit weak fluoresence. Phosphorescence could be detected in the near-infrared for these quinones (even at room temperature), indicating strong spin–orbital coupling and high intersystem crossing efficiency and triplet quantum yield. Theoretical calculations by the INDO method on the triplet energy levels, *assuming planar geometry*, indicate that the lowest triplet energy level in all these quinones is of (π,π*) type. However, the photophysical behavior of 12-methyl-substituted (12-MBAQ) and 7,12-dimethyl-substituted benz[*a*]anthracene-3,4-diones (7,12-DMBAQ) are different from the others. The experimental values of singlet–triplet splitting are much lower (~1000 cm^{-1}) for the above quinones compared to others where it is of the order 3000 cm^{-1}. The above two quinones (12-MBAQ, 7,12-DMBAQ) are capable of H atom abstraction from 2-propanol, indicating that the lowest lying triplet in these cases may indeed be (n,π*) in nature. Thus, our physical/chemical studies show that there is a reversal of state ordering of triplet energy levels compared to theoretical predictions for two quinones, the (n,π*) becoming the lowest triplet state. Such a reversal in the state ordering of triplet energy levels is attributed to the distortion from planar geometry in the above quinones arising from the steric interactions between the methyl hydrogens and the "bay region" phenyl ring hydrogens (the skeletal hydrogen atoms). Steric interaction in the corresponding parent aromatic hydrocarbon has been recently demonstrated by the low-temperature X-ray diffraction studies of the crystal structure of 7,12-dimethylbenz[*a*]anthracene (7,12-DMBA).

The polycyclic aromatic hydrocarbon (PAH) 7,12-dimethylbenz[*a*]anthracene (DMBA) is a potent carcinogen while 7- and 12-MeBA show intermediate activity.[1-4] This is of particular interest because of the presence of two methyl groups in the 7- and 12-positions, which clearly potentiate the carcinogenicity of benz[*a*]anthracene. Recent low-temperature work[3] based on X-ray diffraction studies of DMBA has shown that steric overcrowding in molecules of these types occurs resulting in nonplanarity. DMBA is nonplanar due to steric repulsion in the "bay region"

† University of Houston.
‡ University of Chicago.

(1) Huggins, C. B.; Sugiyama, T. *Proc. Natl. Acad. Sci. U.S.A.* **1966**, *55*, 74–81.
(2) Malaveille, C.; Bartsch, H.; Tierney, B.; Grover, P. L.; Sims, P. *Biochem. Biophys. Res. Commun.* **1978**, *83*, 1468–73.
(3) Huggins, C. B.; Pataki, J.; Harvey, R. G. *Proc. Natl. Acad. Sci. U.S.A.* **1967**, *58*, 2253.
(4) Klein, C. L.; Stevens, E. D.; Zacharias, D. E.; Glusker, J. P. *Carcinogenesis* **1987**, *8*, 5–18.

0002-7863/88/1510-7163$01.50/0

resulting from the close approach of the hydrogen atoms on C(1) and on the methyl group C(12) causing the ring system to deform. The above study also showed that the 7- and 12-positions are highly reactive and appear to show a deficiency of electron density. Aspects of the electronic structure of MeBA's have been investigated by ultraviolet photoelectron spectroscopy.[5]

PAHs must be metabolically activated by the addition of oxygen-containing functional groups in order for them to be carcinogenic.[6-8] It has been shown that certain hydrocarbon quinone metabolites enter into reversible redox cycles involving hydroquinones and semiquinone radicals.[9] In this process, autooxidation of the hydroquinones generates H_2O_2 and other reduced oxygen species that can damage DNA.

For simple *o*-quinones the most important absorption band, from the point of veiw of determining photoreactivity, is the one at the longest wavelength that lies in the region of 500–600 nm (ϵ 20–100). This band is or has been assigned as due to an $n \rightarrow \pi^*$ singlet–singlet transition.[10] The simple *o*-quinones such as 1,2-benzoquinone show weak $n \rightarrow \pi^*$ bands in the visible region. The longest wavelength band of 9,10-phenanthrenequinone occurs in the 500-nm region and is also due to an $n \rightarrow \pi^*$ transition.[11]

The $n \rightarrow \pi^*$ band is sensitive to solvent. For example, 1,2-benzoquinone in ether shows fine structure that is lost in benzene due to a charge-transfer π-complex, and the band system then extends beyond 700 nm.[12] Fluorescence does not commonly occur in *p*- and *o*-quinones. Almost complete intersystem crossing takes place from the lowest n,π^* singlet state ultimately to a lowest n,π^* triplet state from which phosphorescence occurs. The compound 9,10-phenanthrenequinone illustrates this behavior. No fluorescence was observed for 9,10-phenanthrenequinone.[13] Also, 9,10-phenanthrenequinone exhibits a singlet–triplet crossing efficiency of unity, and the triplet level was found to be at $\sim 50 \pm 0.5$ kcal/mol (17 486 cm^{-1}).[13] The n,π^* triplet, owing to its biradical nature, is known to abstract an H atom from alcohols.

o-Quinones are strikingly colored (blue or purple) compounds. No spectroscopic studies have been made on the above benz[*a*]anthracenediones/quinones (BAQ's). In this publication we report the results of photophyscial and photochemical studies made on various methyl-substituted and unsubstituted benz[*a*]anthracene-3,4-diones involving laser flash photolysis, steady-state emission and emission lifetimes, as well as state assignments and theoretical calculations and their comparison with experimental results. The compounds studied were benz[*a*]anthracene-3,4-dione (**1a**, BAQ), 12-methylbenz[*a*]anthracene-3,4-dione (**1b**, 12-MBAQ), 7-methylbenz[*a*]anthracene-3,4-dione (**1c**, 7-MBAQ), and 7,12-dimethylbenz[*a*]anthracene-3,4-dione (**1d**, 7,12-DMBAQ). The dashed area in the structure is termed the bay region.

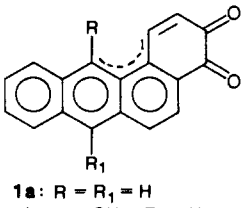

1a: R = R_1 = H
b: R = CH_3, R_1 = H
c: R = H, R_1 = CH_3
d: R = CH_3, R_1 = CH_3

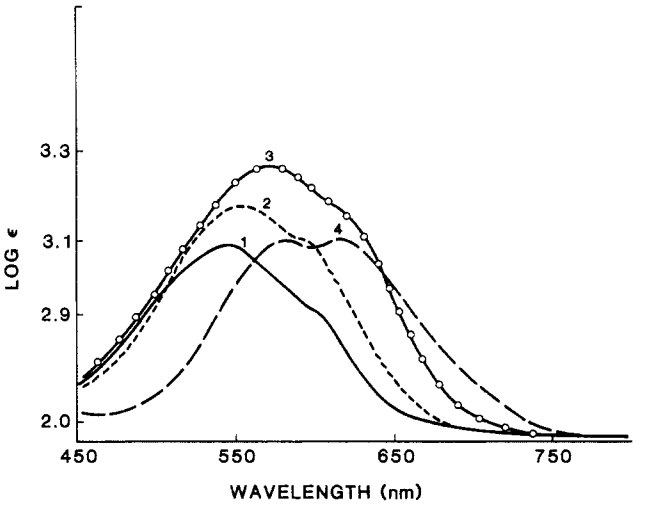

Figure 1. Visible absorption spectra of benz[*a*]anthracene-3,4-diones in benzene: 1, BAQ; 2, 7-MBAQ; 3, 12-MBAQ; 4, 7,12-DMBAQ.

Experimental Section

The quinone 7,12-dimethylbenz[*a*]anthracene-3,4-dione was obtained from Prof. Melvin Newman. The synthesis of this quinone is outlined in ref 14. Syntheses of the other diones are described in ref 15 and 16.

The microsecond laser flash experiments were carried out with a Q-switched Nd:YAG laser (11-ns pulse width). The excitation source was the 532-nm second harmonic. The kinetic absorption spectrometer used to detect optical density (OD) changes after excitation has been described previously.[17] The detection limit of the kinetic system was approximately 200 ns. The solutions were examined in rectangular quartz cell with a 5-mm path length along the monitoring light path and degassed by bubbling nitrogen (also oxygen was used). To record the long-wavelength difference absorption spectrum (700–1100 nm), a silicon diode detector system was used. Fluorescence lifetimes were determined by using a single photon counting technique. The excitation source was a Nd:YAG mode-locked laser pumping at 532 nm (60-ps pulse) and a dye laser tunable from 680 to 780 nm that was frequency doubled. Typically, the frequency-doubled light was less than 1 μW average power. The steady-state phosphorescence measurements were done on a home-made system equipped with a liquid nitrogen cooled germanium diode detector. The excitation was at 365 nm.

Calculations of the intermediate neglect of differential overlap (INDO) type were performed with the INDO/S-Cl model.[18,19] The configuration interaction (CI) consisted of 196 selected single excitations. The two-center electron repulsion integrals were estimated by the Pariser–Parr[20] approximation for the triplet-state calculations. The lengths of all the bonds in the benzene rings for the benzanthracene quinone were assumed to be 1.4 Å. The bond lengths for the *o*-benzoquinone moiety were taken as proposed by Kyboyama et al.[10] for their PPP calculation on *o*-benzoquinone. Our calculations did not take into account any nonplanarity introduced by CH_3–H interaction in substituted BAQ's (all molecules were treated as planar).

Results and Discussion

Figure 1 shows the long-wavelength absorption spectra of benz[*a*]anthracene-3,4-diones in benzene. Table I gives the results of calculations of the $S_0 \rightarrow S_n$ transition energies, intensities, and nature of the transitions by INDO/S method. For comparison, the experimentally observed transition energies and oscillator strengths are also given in Table I. Our calculations show that for all the BAQ's the *lowest* lying *singlet* is of n,π^* nature. This band is not well-defined in the absorption spectra in benzene (Figure 1). Based on both the experimentally observed low intensity and the good agreement between the λ_{max} of the observed low-energy band ($\sim$610 nm) and the n,π^* state assignment by

(5) Akiyama, I.; Harvey, R. G.; Le Breton, P. *J. Am. Chem. Soc.* **1981**, *103*, 6330.
(6) Miller, J. A. *Cancer Res.* **1970**, *30*, 559–76.
(7) Harvey, R. G. *Acc. Chem. Res.* **1981**, *14*, 218.
(8) Dipple, A.; Moschel, R. G.; Bigger, C. A. H. In *Chemical Carcinogenesis*; Searle, C, E.; ACS Monograph 182; American Chemical Society: Washington, DC, 1984.
(9) Loretzen, R. L.; T'so, P. O. P. *Biochemistry* **1977**, *16*, 1467.
(10) Kuboyama, A.; Yamazaki, R.; Yabe, S,; Uehara, Y. *Bull. Chem. Soc. Jpn.* **1969**, *42*, 10.
(11) Kuboyama, A. *Bull. Chem. Jpn.* **1960**, *33*, 1027.
(12) Nagakura, S.; Kuboyama, A. *J. Am. Chem. Soc.* **1954**, *56*, 1003.
(13) Bohning, J. J.; Weiss, K. *J. Am. Chem. Soc.* **1966**, *88*, 2893.
(14) Newman, M. S.; Veeraraghavan, S. *J. Org. Chem.* **1983**, *48*, 3246.
(15) Lee, H.; Harvey, R. G. *J. Org. Chem.* **1986**, *51*, 3502.
(16) Harvey, R. G.; Cortez, D.; Sugiyama, T.; Ito, Y.; Sawyer T. W.; Di Giovanni, J. *Medic. Chem.*, in press.
(17) Lenoble, C.; Becker, R. S. *J. Photochem.* **1986**, *33*, 183.
(18) Ridley, J. E.; Zerner, M. C. *Theor. Chim. Acta* **1973**, *32*, 111.
(19) Ridley, J. e.; Zerner, M. C. *Theor. Chim. Acta* **1976**, *42*, 223.
(20) (a) Pariser, R.; Parr, R. G. *J. Chem. Phys.* **1953**, *21*, 769. (b) Pariser, R. *J. Chem. Phys.* **1952**, *20*, 1499.

Table I. Calculated and Observed $S_0 \rightarrow S_n$ Transition Energies for Benz[*a*]anthracene-3,4-dione and Its Methyl Derivatives

	calcd transition energies				obsd transition energies		
compd	cm^{-1}	nm	*f*	assgnt	cm^{-1}	nm	ϵ, M cm^{-1}
BAQ	15078	663	0.0000	$^1(n,\pi^*)$	16616	600 (sh)	780
	18698	534	0.1660	$^1(\pi,\pi^*)$	18382	544	1210
	22759	439	0.0000	$^1(n,\pi^*)$			
	26614	375	0.0086	$^1(\pi,\pi^*)$	25252	396	3070
	27709	361	0.0560	$^1(\pi,\pi^*)$			
	30570	327	0.1303	$^1(\pi,\pi^*)$	31746	315	~15000
	33608	297	1.2353	$^1(\pi,\pi^*)$			
	36073	277	0.3749	$^1(\pi,\pi^*)$			
7-MBAQ	15104	662	0.0000	$^1(n,\pi^*)$	16501	606 (sh)	1230
	18151	551	0.1606	$^1(\pi,\pi^*)$	17857	560	1470
	22815	438	0.0000	$^1(n,\pi^*)$	24875	402	
	26349	380	0.0244	$^1(\pi,\pi^*)$	26246	381	
	27377	365	0.0480	$^1(\pi,\pi^*)$	28571	350	
	30048	333	0.1488	$^1(\pi,\pi^*)$	31152	321	
	33389	300	1.2658	$^1(\pi,\pi^*)$			
	35533	282	0.2184	$^1(\pi,\pi^*)$			
12-MBAQ	14871	673	0.0000	$^1(n,\pi^*)$	16393	610 (sh)	1520
	18203	549	0.1790	$^1(\pi,\pi^*)$	17543	570	1800
	22379	447	0.0000	$^1(n,\pi^*)$	24390	410	
	26288	380	0.0216	$^1(\pi,\pi^*)$	29239	342	
	27577	363	0.0604	$^1(\pi,\pi^*)$			
	30533	328	0.1389	$^1(\pi,\pi^*)$	31250	320	
	33623	297	1.3515	$^1(\pi,\pi^*)$			
	34496	290	0.0003	$^1(n,\pi^*)$			
	35676	280	0.1195	$^1(\pi,\pi^*)$			
7,12-DMBAQ	14885	672	0.0000	$^1(n,\pi^*)$	16181	618	1310
	17696	565	0.1782	$^1(\pi,\pi^*)$	17036	587	1320
	22392	447	0.0000	$^1(n,\pi^*)$	23923	418	2940
	26103	383	0.0541	$^1(\pi,\pi^*)$	25510	392 (sh)	
	27293	366	0.0545	$^1(\pi,\pi^*)$	27548	363 (sh)	
	30025	333	0.1506	$^1(\pi,\pi^*)$	30488	328	~20000
	33474	299	1.3256	$^1(\pi,\pi^*)$			
	34322	291	0.0004	$^1(n,\pi^*)$			
	34995	286	0.0653	$^1(\pi,\pi^*)$			

theory for a long-wavelength transition near 660–670 nm for these quinones, we assign the bands at ~610 nm, which appear as shoulders, as n,π^* types for all these quinones. This transition would have the n-orbital origin on oxygen of the C=O group.

It is interesting to note that the methyl-substituted quinones 12-MBAQ and 7,12-DMBAQ are blue whereas quinones BAQ and 7-MBAQ are purple. In 12-MBAQ and 7,12-DMBAQ the n,π^* singlet absorption is red-shifted. The adjacent $\pi \rightarrow \pi^*$ transition is also red-shifted, particularly for 7,12-DMBAQ. The ϵ values (Table I) corresponding to the shoulder band are low as expected for n,π^* transition. The ϵ values given are undoubtedly too high since the bands are shoulders on a more intense band except possibly for DMBA (Figure 1). It is worth mentioning that the agreement between the theoretical values of the higher energy transitions of π,π^* type (Table I) and those experimentally determined is also good.

In all these quinones, the two carbonyl groups are adjacent to each other (*o*-quinones) and this well could lead to coupling, resulting in splitting between the two n,π^* (singlet) states. It is seen from Table I that theory does show a splitting, and it has a magnitude of the order of 8000 cm^{-1}; however, for *p*-quinones, such a coupling would be expected to be small and the splitting should be small. For example in anthraquinone, the energy difference between the neighboring n,π^* states is ~2000 cm^{-1}.[21]

Figure 2 shows the difference (ΔOD) transient absorption spectra of the two BAQ's in the wavelength range 380–800 nm (excitation at 532 nm, 11-ns pulse, ~20 mJ) in benzene. Also, the figure has an inset showing the difference absorption spectrum, recorded in a separate experiment in the long-wavelength region 700–1100 nm. The shapes of the ΔOD spectra are similar, and the spectra exhibit maxima around 440 and ~800 nm, with the long-wavelength maximum at 800 nm having high intensity. The minimum intensity in the ΔOD spectra corresponds to the region

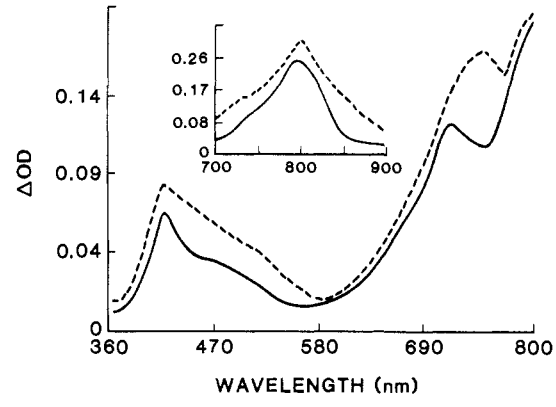

Figure 2. Difference absorption spectra of benz[*a*]anthracene-3,4-diones in benzene (N_2-saturated solution): —, BAQ; ---, 7,12-DMBAQ. Inset: The long-wavelength difference absorption spectrum of the above quinones. All spectra recorded 300 ns after the flash ($\lambda_{excitation}$ = 532 nm).

of $S_0 \rightarrow S_n$ absorption, indicating ground-state depletion.

The transient spectrum in benzene for all these quinones may be assigned as due to the triplet–triplet absorption originating from the T_1 state of the quinones due to the following reasons. The lifetime of the transients for all these quinones at ~440 and ~880 nm were the same and were of the order of 1.5 μs in the case of 12-MBAQ and 7,12-DMBAQ and 4 μs in the other quinones. For all the quinones, substantial quenching by oxygen (~90%) was seen with lifetimes reduced to 0.2–0.3 μs. Finally, energy-transfer experiments with β-carotene in the case of BAQ and 7-MBAQ demonstrated the buildup of the β-carotene triplet at 510 nm clearly arising from T–T energy transfer from the BAQ's to β-carotene.

As noted above, the quinones (12-MBAQ) and (7,12-DMBAQ) showed shorter triplet lifetimes from those of the other two. Addition of 2-propanol (0.1 M) did not affect the triplet decay

(21) Tushighvili, L. Sh.; Shcheglova, N. A.; Shigorin, D. N.; Dokurikhin, N. S. *Russ. J. Phys. Chem.* **1969**, *43*, 542.

Table II. Photophysical Data of Substituted Benz[*a*]anthracene-3,4-diones in Benzene

compd	longest abs max, nm	fluorescence max, nm	fluorescence lifetime, ns	phosphorescence max, nm	triplet lifetime (τ), μs	T–T abs max, nm	ΔE_{S_1-T}, cm^{-1}
BAQ	600 (sh)	685		905	4.2	805	2960
	544					420	
7-MBAQ	606 (sh)	720	1	915	4	800	2300
	560					420	
12-MBAQ	610 (sh)	735	0.5	915	1.8	820	1500
	570					420	
7,12-DMBAQ	618	740		920	1.5	800	960
	587					420	

Table III. Calculated and Observed Triplet Energy Levels for Benz[*a*]anthracene-3,4-dione and Its Methyl Derivatives

compd	calcd triplet energy levels, cm^{-1} (λ, nm)	state	obsd[a] lowest triplet, cm^{-1} (λ, nm)
BAQ	11372 (879)	$^3(\pi,\pi^*)$	11050 (905)
	16110	$^3(n,\pi^*)$	
	18290	$^3(\pi,\pi^*)$	
	27669	$^3(\pi,\pi^*)$	
7-MBAQ	11054 (904)	$^3(\pi,\pi^*)$	10930 (915)
	16157	$^3(n,\pi^*)$	
	18085	$^3(\pi,\pi^*)$	
	27236	$^3(\pi,\pi^*)$	
12-MBAQ	10660 (938)	$^3(\pi,\pi^*)$	10930 (915)
	15893	$^3(n,\pi^*)$	
	18236	$^3(\pi,\pi^*)$	
	27463	$^3(n,\pi^*)$	
7,12-DMBAQ	10300 (970)	$^3(\pi,\pi^*)$	10870 (920)
	15931	$^3(n,\pi^*)$	
	17968	$^3(\pi,\pi^*)$	
	27476	$^3(\pi,\pi^*)$	

[a] These observed values are taken as the maximum of the phosphorescence spectra experimentally observed.

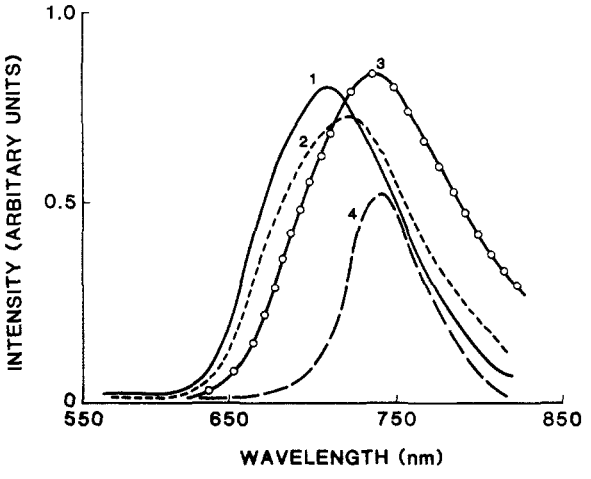

Figure 3. Steady-state fluorescence spectra of benz[*a*]anthracene-3,4-diones in benzene: 1, BAQ; 2, 7-MBAQ; 3, 12-MBAQ; 4, 7,12-DMBAQ. The wavelength of excitation corresponded to the maximum of the lowest singlet absorption band (Table II) of the respective quinone.

of quinones BAQ and 7-MBAQ, whereas in the case of 12-MBAQ and 7,12-DMBAQ the triplet decay was faster with lifetimes of 0.33 and 0.25 μs, respectively. In addition to the fast triplet decay, a slow-decay component peaking around 480 nm was seen for both 12-MBAQ and 7,12-DMBAQ. This slow decay gave a good fit for a second-order kinetic process ($k_2 = 1.5 \times 10^6$ M s^{-1}). The above observations are indicative of H atom abstraction from 2-propanol by the triplet of quinones 12-MBAQ and 7,12-DMBAQ to yield radicals 12-MBAQH and 7,12-DMBAQH, respectively. The slow decay corresponds to that the foregoing semiquinone radicals. These two quinones were capable of H atom extraction even from toluene (methyl group) as seen by the presence of a slow decay in addition to the fast-decaying triplet. The H abstraction implies that the lowest triplet energy level in these quinones may indeed be of n,π^* nature, since n,π^* triplets because of their biradical nature are known to absract H from alcohols. In contrast, the quinones BAQ and 7-MBAQ did not abstract H even in 100% 2-propanol. Hence, for BAQ and 7-MBAQ, the lowest lying triplet energy level must be of π,π^* type and not n,π^*. Table III gives the theoretical calculations of the triplet energy levels of the quinones by the INDO/S-CI model. *Planar geometry* has been *assumed* for all the quinones. The calculations show that, for all the quinones, the lowest lying triplet is of π,π^* nature. The experimental results show that, in the case of quinones 12-MBAQ and 7,12-DMBAQ, the lowest triplet is of n,π^* nature and does not agree with the calculations. This dictates a reversal of state ordering from that calculated and strongly suggests that the assumption of planarity used for the calculations for these two compounds is not correct; see later discussion.

We also observed phosphorescence emission in benzene at room temperature in the 900–920-nm region for all these quinones (Table II). By bubbling in oxygen, we observed the singlet oxygen emission ($^1\Delta_g$) at ~1270 nm, formed by energy transfer from the triplet of the quinones. It can be seen from Table III that there is good agreement between the experimental λ_{max} of the phosphorescence spectra and the calculated values.

Fluorescence generally occurred in the 685-740-nm region, and the intensity, in general, was weak ($\Phi_F \leq 0.05$) (Figure 3). The photophysical characteristics of these quinones seem to follow the general pattern of other quinones. The weak fluorescence, short fluorescence lifetime (we could not measure the fluorescence lifetime in the case of BAQ and 7,12-DMBAQ because the intensity was too weak), and observation of phosphorescence at room temperature point to large spin–orbital coupling, giving high intersystem crossing efficiency and triplet quantum yield. We attempted to estimate the magnitude of the extinction coefficient of the triplet in one case, the unsubstituted quinone BAQ, by energy transfer with β-carotene. The ϵ was of the order of 70000 M cm^{-1} (λ = 770 nm).

It has been shown[4] recently, based on X-ray diffraction studies at low temperature (180 K), that polycyclic aromatic hydrocarbons having no methyl group in the bay region are very nearly planar (torsion angles less than 2° in the bay region). Substitution of a methyl group in the 12-position in the bay region in benz[*a*]-anthracene structures results in a highly hindered and nonplanar geometry for the molecules owing to the steric repulsive interaction between the methyl hydrogens and the hydrogen of the angular benzene ring in the bay region. This results in the twisting of the polycyclic aromatic carbon skeleton to minimize the intramolecular interactions between the methyl hydrogen atoms and the skeletal hydrogen atoms leading to distortion from planar geometry (also see ref 22 for a comprehensive review on structural and other aspects of aromatic hydrocarbons). Such a distortion could also occur in these sterically hindered bay region quinones affecting the delocalization properties of the π-electrons and lead to reversal in the order of the triplet energy levels for the quinones 12-MBAQ and 7,12-DMBQ (n,π^* state lowest). This idea seems highly feasible since the energy levels of the lowest lying π,π^* and

(22) Glusker, G. In *Polycyclic Hydrocarbons and Carcinogenesis*; Harvey, R. G., Ed.; ACS Monograph 283; American Chemical Society: Washington, DC, 1985; pp 125–85.

neighboring n,π^* are not far apart in a planar configuration as shown by our calculations (Tables I and III).

Further support for the lowest triplet energy level of 12-MBAQ and 7,12-DMBAQ being n,π^* may be derived from the experimental S_1–T_1 splitting energy values. The magnitude of splitting is low for the latter quinones ($\sim$1000 cm^{-1}), which is of the order of splitting for $S_{(n,\pi^*)}$–$T_{(n,\pi^*)}$ in quinones. For the other quinones, this splitting is 2–3-fold greater. Also, the substantial red-shift in the visible absorption bands (Figure 1) of 12-MBAQ and 7,12-DMBAQ may be due to the consequences of the distortion discussed earlier. Finally, it is easy to explain the behavior of the quinone 7-MBAQ being very similar to the unsubstituted quinone. Here the methyl substitution is far away from the bay region and very probably has no consequence on the planarity of the ring structure.

Registry No. 1a, 74877-25-1; **1b**, 111238-10-9; **1c**, 71989-02-1; **1d**, 70092-13-6.

Chemistry of Singlet Oxygen. 51. Zwitterionic Intermediates from 2,4-Hexadienes

Kevin E. O'Shea and Christopher S. Foote*

Contribution from the Department of Chemistry and Biochemistry, University of California, Los Angeles, California 90024. *Received March 14, 1988*

Abstract: The three isomeric 2,4-hexadienes give nearly identical product distributions with singlet oxygen. Singlet oxygen causes rapid interconversion of the isomers, and methoxy hydroperoxides are formed from all three dienes in methanol (*E,Z* and *Z,Z* ~25%, *E,E* <10%). These observations are explained by intermediate zwitterions that revert to isomerized dienes in competition with collapse to products or capture by methanol.

Singlet oxygen undergoes Diels–Alder [2 + 4] addition to dienes to give endoperoxides, "ene" reaction with olefins with abstractable allylic hydrogens to give allylic hydroperoxides, and [2 + 2] addition to give dioxetanes.[1] Although details of the reactions are still unclear and numerous mechanisms have been proposed, the Diels–Alder process is widely believed to be a simple concerted reaction. However, methanol adducts formed in the reaction of singlet oxygen with structurally restricted dienes such as 2,4-dimethyl-2,4-hexadiene[2] and indenes[3] provide evidence for nonconcerted pathways involving polar or biradical intermediates. We now report evidence for such intermediates in the reaction of singlet oxygen even with simple dienes.

Results and Discussion

The (*E,E*)-, (*E,Z*)-, and (*Z,Z*)-2,4-hexadienes were photooxidized at −78 °C in CD_2Cl_2 with tetraphenylporphine as sensitizer. The *E,E* isomer gives the expected *cis*-endoperoxide (A) as the major product (Scheme I). However, the *E,Z* isomer also yields the *cis*-endoperoxide as the major product as Gollnick reported.[4] The product distribution from the *Z,Z* isomer is nearly identical with that of the *E,Z* isomer. All three dienes also give a complex mixture of hydroperoxides, acetaldehyde, and *cis*- and *trans*-2-butenal (Table I).

The aldehyde products apparently come from cleavage of dioxetanes. However, attempts to observe dioxetanes or other reactive intermediates by NMR were unsuccessful at −80 °C, even using filtered light (>450 nm), which left the product distribution unchanged. Pure *cis*-endoperoxide (A) was isolated and characterized by several spectroscopic techniques, including DEPT and 2-D NMR experiments (Figure 1). The *trans*-endoperoxide was characterized as a mixture with the cis (Figure 2). The IR and mass spectral data are in accord with those reported by Gollnick[4] and Matsumoto.[5] The *cis*-endoperoxide exhibits temperature-dependent proton and carbon NMR spectra, indicating slow half-chair–half-chair interconversion,[6] coalescing at −50 °C.

The doubly allylic hydroperoxides decompose at room temperature or upon attempted chromatography and were therefore characterized by NMR in product mixtures. The ^{1}H NMR spectra have peaks whose chemical shifts and relative areas are consistent with the assigned structures (broad proton singlets at 8–9 ppm that disappear when methanol is added, complicated multiplets in the vinyl region, and doublets around 2.0 ppm); there are also corresponding peaks in the ^{13}C spectra.

Scheme I

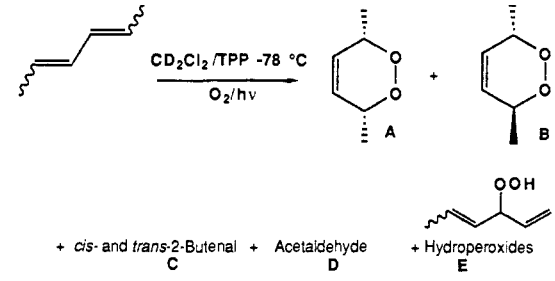

Table I. Products of Photooxidation of 2,4-Hexadienes

	product, %				
isomer	A	B	C	D	E
E,E	74	7	3	4	11
E,Z	46	12	12	8	23
Z,Z	42	10	12	11	25

(1) Review: A. A. Frimer In *Singlet Oxygen*; A. A. Frimer, Ed.; CRC: Boca Raton, FL, 1985; Vol II.
(2) (a) Manring, L. E.; Kanner, R. C.; Foote, C. S. *J. Am. Chem. Soc.* **1983**, *105*, 4707, 4710. (b) Gollnick, K.; Griesbeck, A. *Tetrahedron* **1984**, *40*, 3235.
(3) (a) Fenical, W.; Kearns, D. R.; Radlick, P. *J. Am. Chem. Soc.* **1969**, *91*, 2655, 3396, 7771. (b) Hatsui, T.; Takeshita, H. *Bull. Soc. Chem. Jpn.* **1980**, *53*, 2655.
(4) Gollnick, K.; Griesbeck, A. *Tetrahedron Lett.* **1983**, *24*, 3303.
(5) Matsumoto, M.; Dobashi, S.; Kuroda, K.; Kondo, K. *Tetrahedron* **1985**, *41*, 2147.
(6) $\Delta G^{\ddagger}$ ~10.5 kcal/mol. Similar behavior has been reported for an alkoxy-substituted endoperoxide: Clennan, E. J.; Nagraba, K. *J. Org. Chem.* **1987**, *52*, 294.
(7) Ogilby, P. R.; Foote, C. S. *J. Am. Chem. Soc.* **1983**, *105*, 3423.

0002-7863/88/1510-7167$01.50/0